Chemical Geology 566 (2021) 120103

Contents lists available at ScienceDirect

Chemical Geology

journal homepage: www.elsevier.com/locate/chemgeo

Assessing molybdenum isotope fractionation during continental weathering as recorded by weathering profiles in saprolites and bauxites

Allison T. Greaney [a,1,*], Roberta L. Rudnick [a], Stephen J. Romaniello [b,2], Aleisha C. Johnson [b,3], Ariel D. Anbar [b,c], Michael L. Cummings [d]

[a] University of California - Santa Barbara, Department of Earth Science and Earth Research Institute, Santa Barbara, CA 93106, United States of America
[b] Arizona State University, School of Earth and Space Exploration, Tempe, AZ 85281, United States of America
[c] Arizona State University, School of Molecular Sciences, Tempe, AZ 85281, United States of America
[d] Department of Geology, Portland State University, Portland, OR 97207, United States of America

ARTICLE INFO

Editor: Catherine Chauvel

Keywords:
Molybdenum
Weathering
Isotope fractionation
Continental crust

ABSTRACT

Molybdenum isotopes in three deep and well-characterized weathering profiles – a saprolite formed on metadiabase from South Carolina, USA, and two ferruginous bauxites formed on Columbia River Basalts in Oregon and Washington, USA – elucidate Mo isotope behavior during continental weathering. The saprolite records an overall loss of Mo relative to the fresh bedrock, as indicated by negative τ^{Mo}_{Ti}, which defines the loss of Mo relative to the relatively immobile element Ti. The saprolites are also isotopically light: δ^{98}Mo values range from −0.89‰ (relative to NIST 3134) to −0.05‰, mean $\delta^{98}Mo = -0.40‰$, compared to $+0.55‰_{NIST3134}$ for the underlying unweathered bedrock. By contrast, the ferruginous bauxites generally record addition of Mo relative to the fresh bedrock (zero to positive τ^{Mo}_{Ti}) and generally have higher δ^{98}Mo values than the parental basalts: δ^{98}Mo of the bauxites range from −0.14‰ to +0.38‰ compared to −0.33‰ and +0.02‰ for the unweathered parental basalt. Low δ^{98}Mo values in the saprolites likely reflect preferential retention of isotopically light Mo adsorbed onto accessory Fe-oxy-hydroxides and clays during weathering, whereas the high δ^{98}Mo values in the bauxites reflect the addition of isotopically heavy Mo from groundwater. When the three profiles are combined, there is a positive correlation between τ^{Mo}_{Ti} and δ^{98}Mo, suggesting that when Mo is lost during continental weathering, the resulting regolith is isotopically light, whereas groundwater addition can shift the regolith to heavier values. Because saprolites are a more common weathering product than bauxites, we conclude that, in general, continental weathering fractionates Mo isotopes such that the weathered upper crust retains isotopically light Mo. In contrast, the groundwater that leaches Mo from the weathered crust is isotopically heavy. Thus, chemical weathering of continents generates the isotopically heavy riverine signature observed globally, and partially contributes to the isotopically heavy seawater signature. Finally, these data, in conjunction with previously published data for glacial diamictites, can be used to assess changes in the crustal Mo isotope signature over the last 2.9 Ga.

1. Introduction

Molybdenum (Mo) isotopes are increasingly used as a paleo-redox proxy because isotope signatures in the sediments of a marine basin can elucidate the redox chemistry of the water column. However, these studies rely on assumptions about the Mo isotope signature of the Mo source to the basin, which may differ from that of average crustal rocks. Generally, paleo-redox studies leverage the Mo isotope composition of marine sediments to determine the chemical state of the oceans or atmosphere at the time of deposition (e.g., Kendall et al., 2017 and references therein). Molybdenum isotope fractionation may also occur during continental weathering, thus altering the input signature to the water column from that of average upper continental crust. This fractionation may be an important step in generating the Mo isotope

* corresponding author.
E-mail address: greaneyat@ornl.gov (A.T. Greaney).
[1] Now at Oak Ridge National Laboratory, Oak Ridge, TN 37830.
[2] Now at University of Tennessee Knoxville, Department of Earth and Planetary Sciences, Knoxville, TN 37996.
[3] Now at University of Chicago, Department of the Geophysical Sciences, Chicago, IL 60637.

https://doi.org/10.1016/j.chemgeo.2021.120103
Received 31 August 2020; Received in revised form 30 December 2020; Accepted 26 January 2021
Available online 1 February 2021

signatures of marine sediments. For example, modern average river water (δ^{98}Mo = +0.7; Archer and Vance, 2008) is isotopically heavier than igneous continental crust (average between +0.05 and + 0.20‰; Voegelin et al., 2014; Willbold and Elliott, 2017; Yang et al., 2017). This offset has been attributed to fractionation that occurs within seawater or river water (e.g., isotopically light Mo adsorbs onto Fe—Mn oxides and nodules; Barling and Anbar, 2004; Siebert et al., 2003) and/or during continental weathering (Archer and Vance, 2008; Pearce et al., 2010; Greaney et al., 2020). This study aims to determine the nature of Mo isotope fractionation during continental weathering.

1.1. Mo isotope fractionation in weathering profiles

Secondary minerals and organic compounds that form during continental weathering may sequester Mo in deep soil profiles. Iron-manganese oxyhydroxides (shortened to Fe—Mn oxides) are known to preferentially adsorb light Mo isotopes, leaving heavier isotopes in solution. This behavior was first observed in oxic pelagic sediments (Siebert et al., 2003; Barling et al., 2001) and has since been demonstrated experimentally through adsorption of Mo onto goethite, magnetite, hematite, ferrihydrite, and birnessite (Barling and Anbar, 2004; Goldberg et al., 2009; Wasylenki et al., 2008; Wang et al., 2020). In the modern environment, Mo isotope fractionation by adsorption onto oxides is a significant global process, resulting in large fractionations in the marine environment and potentially the terrestrial environment (Wang et al., 2018; Greaney et al., 2020).

In addition to Fe—Mn oxides, organic carbon also serves as an important scavenger of Mo and also leads to isotopic fractionation within shallow soils (Chappaz et al., 2014; Dahl et al., 2017). In studies of forest soils, Wichard et al. (2009) found that ~25% of Mo is complexed by organic matter in the organic-rich topsoil, while Marks et al. (2015) found that, on average, 33% of bulk soil Mo is complexed onto organic matter. When molybdate (MoO_4^{2-}, the dominant Mo compound in oxidized waters) complexes with leaf litter, for example, Mo changes coordination state from tetrahedral to octahedral (Wichard et al., 2009), and one might presume that an isotope fractionation would accompany such a change. A positive correlation between δ^{98}Mo and organic carbon abundance in Hawaiian soils (King et al., 2016) suggests that organic matter incorporates heavy Mo isotopes, thus inducing the opposite fractionation as Fe,Mn-oxides. By contrast, King et al. (2018) showed experimentally that humic acid, which forms by decay of plant and animal matter in soils, absorbs lighter Mo isotopes, much like the fractionation that is observed for Fe—Mn oxide adsorption. King et al. (2018) attributed the heavy Mo isotope signatures of the Hawaiian soil profiles to late addition of isotopically heavy atmospheric Mo (e.g., from rainwater and volcanic fog) that binds to organic matter. These studies, which highlight the potential importance of organic matter, were all performed in relatively shallow soil settings.

Other studies have taken a more comprehensive approach to characterizing Mo isotope fractionation in shallow, organic-rich soils. Siebert et al. (2015) measured Mo isotope values in three weathering profiles from Hawaii, Puerto Rico, and Iceland and found that redox conditions, organic matter, Fe—Mn oxides, degree of weathering, pH, atmospheric inputs, climate, and parent rock type may all influence Mo isotope fractionation during chemical weathering, and suggested that weathering may have a significant influence on the global Mo isotope cycle. They also found that soils that show a net Mo loss retain light Mo isotopes relative to the parent rock, while soils showing a net Mo gain are offset to heavier isotopic values than the parent material. Molybdenum concentration is correlated with organic matter in soils that show a net Mo gain.

In the absence of abundant Fe—Mn oxides or organic matter, there are other mechanisms by which Mo isotopes may be fractionated in deep soil profiles. Aluminum hydroxides (e.g., gibbsite) and some clays (e.g., montmorillonite) are capable of adsorbing Mo at low pH and may also play a role in Mo isotope fractionation during continental weathering (Goldberg et al., 1996). This was observed by Wang et al. (2018) who found that aluminum hydroxides and, to a lesser extent, clays likely retain isotopically light Mo in saprolites. Later work of Wang et al. (2020) found that in laterite profiles, residual, light Mo isotopes are retained within primary Fe—Ti oxides that are resistant to weathering.

The pH of the soil plays an important role in overall Mo adsorption, no matter the adsorbing phase. Goldberg et al. (1996) showed that nearly 100% of Mo is retained in acidic soils at a pH < 4, whereas no retention was found to occur at pH > 8.

Overall, Fe—Mn oxides, organic matter, pH of the soil, and atmospheric inputs may all influence Mo isotope fractionation during continental weathering; however, more work is necessary to determine the relative roles of these variables in modern weathering environments, especially in deep soil profiles that are less pervasively impacted by biology.

1.2. Reconciling temporal Mo trends with weathering patterns

A global shift in the geochemical behavior of Mo is observed across the Archean-Proterozoic boundary, coinciding with the great oxidation event (GOE) at ~2.4 Ga (Anbar et al., 2007; Scott et al., 2008; Greaney et al., 2020). It is hypothesized that the rise of O_2 resulted in the enhanced weathering of crustal Mo-bearing sulfides (Johnson et al., 2019) and subsequent release of soluble Mo^{6+} from the crust. Black shales record evidence of this process at 2.5 Ga and potentially earlier in the form of elevated authigenic Mo enrichments and a shift to higher δ^{98}Mo values, indicating an elevated seawater Mo reservoir and enhanced burial of Mo in oxide-bearing sediments (Siebert et al., 2005; Anbar et al., 2007; Wille et al., 2007; Scott et al., 2008; Duan et al., 2010; Wille et al., 2013; Ostrander et al., 2019). Contemporaneous Mo depletion and isotopic fractionation towards lower δ^{98}Mo values are observed in glacial diamictites that sample weathered upper continental crust at this time, suggesting the weathered continental crust may be a complementary, isotopically light Mo reservoir to the isotopically heavy values of ancient seawater (Gaschnig et al., 2014; Greaney et al., 2020).

In this paper, we present Mo concentrations and isotope data for deep weathering profiles of saprolite and bauxite to understand how Mo behaves during different styles of weathering of continental crust. The saprolite data support the conclusions of previous studies (e.g., Wang et al., 2018) that Mo is leached and becomes isotopically lighter in saprolites; the bauxite data are the first Mo isotope data to be presented for this lithology. We use these data along with literature data to determine whether continental weathering can explain the shift in Mo isotope composition of the weathered upper continental crust recorded by glacial diamictites over the last ~3 Ga (Greaney et al., 2020) and to test the hypothesis of Archer and Vance (2008) that continental weathering contributes to the isotopically heavy riverine Mo signature.

1.3. Samples

To assess the influence of chemical weathering on Mo isotopes, we analyzed weathering profiles through a saprolite and two bauxites that represent the chemical breakdown of igneous bedrock under different weathering conditions. Saprolites form under relatively moderate weathering conditions where clays are the stable and dominant mineral species, whereas bauxites form under intense leaching conditions in the presence of added rainwater or groundwater where Si is removed (Schellmann, 1994). The saprolites and bauxites studied here were originally collected and characterized by Gardner (1981) and Fassio (1990), respectively.

Seventeen samples from a saprolite profile that formed on a metadiabase in South Carolina were selected for analyses. The samples span 11 m in depth and were collected from an outcrop exposed in the wall of a quarry (Gardner, 1981). The saprolites formed in the Tertiary in a subtropical climate; the current mean annual precipitation (MAP) is 1200 mm/yr with a current mean annual temperature (MAT) of 18 °C

(Gardner, 1981; Rudnick et al., 2004). The saprolites formed on a diabase dike that experienced greenschist facies metamorphism, as recorded by the significant abundance of talc and chlorite (Rudnick et al., 2004). The saprolites are primarily composed of kaolinite and smectite, as determined by XRD (Gardner, 1981). A redox discontinuity is observed at ~2 m depth, above which Fe-rich smectite formed in a relatively oxidizing environment, and below which kaolinite is the dominant assemblage reflecting more reducing conditions. Siderite boxwork veins are found just below the 2 m discontinuity, suggesting that reducing conditions allowed Fe to become soluble. These saprolites have been previously analyzed for Li, Mg, K, Fe, and Cu isotopes (Liu et al., 2014a; Rudnick et al., 2004; Teng et al., 2010; Teng et al., 2020). The Cu and Fe isotope data suggest that Fe-oxides formed by the oxidation of siderite in the uppermost 2 m of the profile, scavenging light Fe and heavy Cu isotopes (Liu et al., 2014a).

Eight samples from each of two bauxite weathering profiles are studied here. The bauxites developed on ~16 Ma Columbia River Basalts on the western and rainy side of the Cascade Mountains in Columbia County, Oregon, and Cowlitz County, Washington. All samples come from drill core (Fassio, 1990). The present day MAP is ~1100 mm/yr and MAT is ~11 °C (Liu et al., 2013; Western Regional Climate Center), however it is likely that the bauxites formed in a warmer and more humid environment (between 13 °C and 18 °C; Kohn et al., 2002). The eight samples span each bauxite profile, named Columbia and Cowlitz, to ~8 m depth. As the drill cores did not penetrate fresh basalt, the parental basalts were collected elsewhere (see details in Liu et al., 2013). The bauxites are composed of gibbsite, halloysite, kaolinite, hematite, goethite, maghemite, and the uppermost samples contain quartz, as determined by XRD (Liu et al., 2013; Fassio, 1990). The bauxite profiles can be divided into two major zones: an upper zone containing varying proportions of iron pisolites (Supplementary Fig. S1), and a lower zone composed of nodular gibbsite (Fassio, 1990). This separation into a ferruginous layer overlying an aluminous layer is a common feature of bauxite deposits (Schellmann, 1994; Bogatyrev et al., 2009). Both profiles have been previously analyzed for Li, Mg, K, and Nd isotopes (Liu et al., 2013; Liu et al., 2014b; Chen et al., 2020). Lithium and K isotope fractionation was observed in all profiles, resulting in offset to lighter δ^7Li and δ^{41}K values. Net Mg fractionation was also observed in all profiles, resulting in offset to heavier δ^{26}Mg values. However, Liu et al. (2013) also determined that aeolian dust was added to the upper 3 m of the bauxites, as documented by the presence of quartz and less radiogenic Nd isotopes. The dust did not significantly affect the δ^7Li signature, but did add isotopically light Mg and heavy K to the top 3 m of the profiles (Liu et al., 2013; Liu et al., 2014b; Chen et al., 2020).

2. Methods

Mo isotope and trace element analyses were carried out in the W.M. Keck Foundation Laboratory for Environmental Biogeochemistry at Arizona State University. Molybdenum and other trace element concentrations were measured on an iCAP Quadropole ICP-MS with data reduction done by calibrating counts per second (CPS) relative to synthetic standard solutions. Precision on Mo concentration [Mo] is generally better than 8%. Molybdenum isotopes were analyzed using a Mo double spike method and a Neptune MC-ICP-MS. Methods follow that of Romaniello et al. (2016) and Greaney et al. (2020) and are described in the supplementary information. Molybdenum isotope data are reported as $\delta^{98}Mo = 1000*[(^{98}Mo/^{95}Mo_{sample})/(^{98}Mo/^{95}Mo_{standard})-1]$, using the NIST 3134 standard. The USGS standard SDO-1, a Devonian shale, was dissolved and run alongside the samples to assess data quality. SDO-1 shows excellent reproducibility of literature values, with an average δ^{98}Mo value of +0.79‰ ± 0.03. All uncertainties are reported as 2σ. Long-term reproducibility is 0.04‰.

3. Results

3.1. Saprolites

The saprolites contain between 0.21 and 1.69 ppm Mo, with an average of 0.46 ppm. Their δ^{98}Mo values range between −0.89‰ and −0.05‰, with an average of −0.40‰ (Table 1). Sample M20 is estimated to be the best representative of the unweathered, metamorphosed diabase bedrock and contains 0.60 (±0.05) ppm Mo with a δ^{98}Mo of +0.55‰. There is no systematic variation in [Mo] or isotope fractionation with depth in the profile, with the exception of the samples that lie at or above the 2 m redox discontinuity (Fig. 1). In Fig. 1 and subsequent figures, the five saprolite samples that lie above the redox discontinuity (e.g., in the more oxidizing environment) are shaded darker to denote the different redox environment that they formed in.

Molybdenum mobility during weathering is calculated as tau (τ) relative to less mobile element Ti, where WP = weathering profile and BR = bedrock in the following calculation:

$$\tau_{Ti}^{Mo} = \left(\frac{Mo_{WP} * Ti_{BR}}{Ti_{WP} * Mo_{BR}}\right) - 1 \quad (1)$$

Positive τ values indicate that Mo was gained relative to Ti, while negative τ values indicate that Mo was lost. All saprolite samples, save three, lost Mo (Fig. 2). The three samples that gained Mo sit at the redox-interface between 2 and 3 m depth.

Table 1
Molybdenum concentration and isotope data for the three profiles studied here. BR stands for bedrock.

	Depth (m)	δ^{98}Mo	2σ	Mo (ppm)	2σ	τMo - Ti	$\Delta^{98}Mo_{BR-WP}$
SDO-1		0.79	0.03	154	11.7		
Saprolites							
M1	0.10	−0.56	0.05	0.21	0.02	−0.63	1.10
M3	0.50	−0.05	0.06	0.41	0.03	−0.44	0.60
M4	1.00	−0.06	0.08	0.38	0.03	−0.18	0.61
M5	1.50	−0.57	0.14	0.68	0.05	0.31	1.12
M6	2.00	−0.34	0.05	0.75	0.06	0.25	0.88
M7	3.00	−0.05	0.05	1.69	0.13	0.99	0.59
M8	4.00	−0.51	0.06	0.51	0.04	−0.39	1.06
M9	5.00	−0.89	0.05	0.28	0.02	−0.65	1.44
M10	6.00	−0.58	0.06	0.38	0.03	−0.51	1.13
M11	7.00	−0.23	0.01	0.27	0.02	−0.58	0.78
M12	8.00	−0.16	0.04	0.29	0.02	−0.57	0.71
M13	9.00	−0.35	0.03	0.28	0.02	−0.64	0.90
M14	10.0	−0.63	0.04	0.32	0.02	−0.60	1.17
L14-8	10.0	−0.16	0.02	0.42	0.03	−0.34	0.70
L14-9	10.0	ND	ND	0.25	0.02	−0.59	0.55
M15	11.0	−0.83	0.07	0.27	0.02	−0.65	1.38
M20-BR		0.55	0.01	0.60	0.05		
Columbia							
514	2.74	0.19	0.01	5.57	0.42	3.76	0.52
516	3.96	0.19	0.00	6.09	0.46	3.44	0.52
518	4.57	0.14	0.03	7.83	0.59	2.74	0.47
5110	5.49	0.26	0.04	16.5	1.26	3.57	0.59
5112	6.71	0.34	0.02	12.0	0.91	3.56	0.67
5114	7.32	−0.09	0.04	3.49	0.27	0.07	0.24
5115	7.92	−0.14	0.04	3.03	0.23	−0.04	0.20
POM - BR		−0.33	0.11	0.73	0.06		
Cowlitz							
931	2.13	0.28	0.05	4.66	0.35	1.67	0.27
933	2.74	0.38	0.05	8.03	0.61	2.75	0.37
9310	5.79	−0.13	0.06	1.76	0.13	−0.11	0.14
9319	6.25	−0.10	0.07	1.51	0.12	−0.11	0.12
9321	7.62	−0.07	0.02	1.44	0.11	−0.23	0.08
9322	8.23	0.00	0.06	1.97	0.15	0.03	0.01
9323	9.14	−0.16	0.06	1.23	0.09	−0.30	0.18
SB1- BR		0.02	0.02	0.90	0.07		

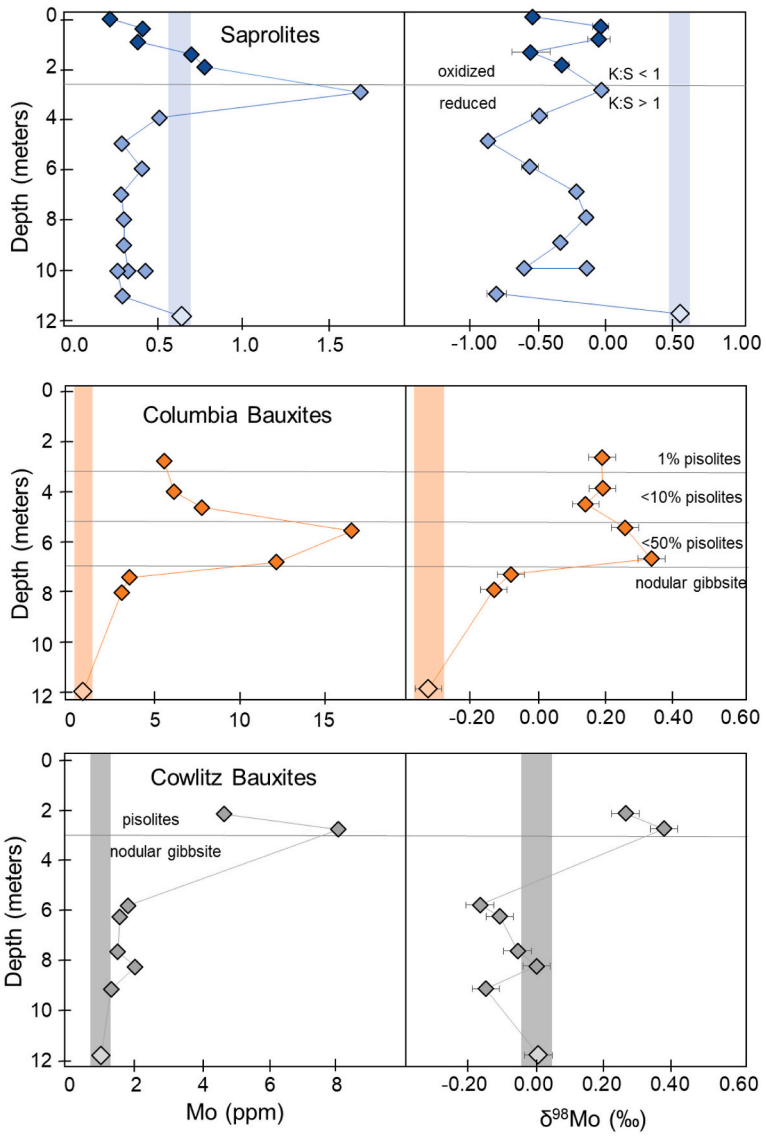

Fig. 1. Variations in Mo concentration and isotope fractionation with depth. The bedrock is plotted at 12 m for clarity on the diagram but may be found lower in the profile. In the case of the bauxites, fresh bedrock was not encountered in the drill hole, so fresh basalts of the same member were sampled elsewhere. In the saprolite profile, the kaolinite:smectite ratio change is denoted by K:S, and the iron pisolite and gibbsite layers are delineated in the bauxite profiles. The shaded bars represent the unweathered bedrock δ^{98}Mo value.

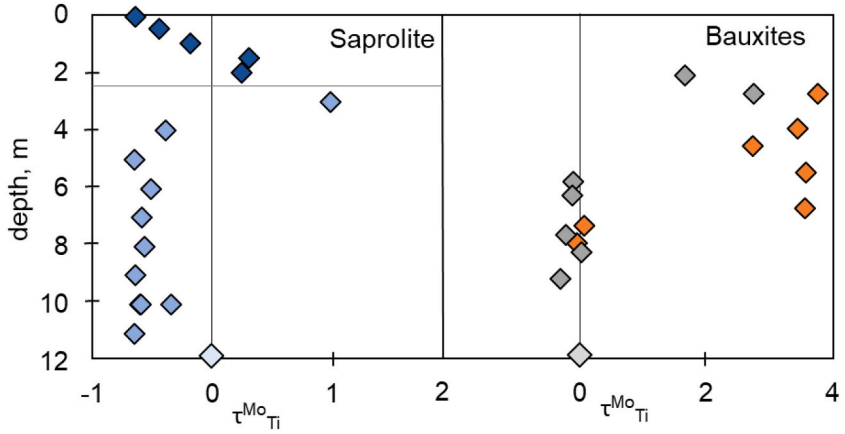

Fig. 2. Calculated τ values as a function of depth in the saprolite profile (left) and bauxite drill cores (right). These show Mo addition in both profiles at certain horizons. The horizontal line in the saprolite profile at ~2 m denotes a redox discontinuity and a change in kaolinite:smectite ratio. See text for definition of τ.

3.2. Bauxites

The bauxites contain between 1.23 and 16.5 ppm Mo, with an average of 5.37 ppm. The bauxite δ^{98}Mo values range between −0.14 and +0.38‰, with an average of +0.08‰ (Table 1). POM and SB-1 are the fresh parent basalts for the two bauxite profiles and contain 0.73

(±0.06) and 0.90 (±0.07) ppm Mo with isotopic signatures of −0.33‰ and +0.02‰, respectively. In the Columbia samples (orange, Fig. 1), there is an excursion to higher concentrations and higher δ^{98}Mo values above 7 m depth. Similarly, in the Cowlitz profile (gray, Fig. 1), the uppermost two samples show higher [Mo] and heavier Mo isotopes. The τ calculations show that the lower gibbsite layers of the two profiles have normalized [Mo] similar to the parent basalts, however the samples from the overlying iron-pisolite layers have gained Mo (Fig. 2).

4. Discussion

4.1. Saprolites

The saprolite data show an overall loss of Mo and selective retention of lighter Mo isotopes relative to the parent rock. While there are no systematic trends within either [Mo] or δ^{98}Mo, there are several interesting features in the dataset. First, Mo shows varying behavior on either side of the redox discontinuity at ~2 m depth. Above this discontinuity, where Fe-rich smectite is the dominant clay species and the environment is likely more oxidizing, [Mo] follows a continuous trend of decreasing concentration towards the top of the profile (Figs. 1, 2). Molybdenum may be mobilized in the oxidized zone, migrate downwards, and accumulate along the discontinuity as it comes into contact with the reducing environment where siderite precipitated. In the upper oxidized zone, there is a weak correlation between [Mo] and P_2O_5 (Supplementary Fig. 2), which has been shown to compete with Mo for adsorption sites on the surfaces of minerals (Goldberg et al., 1996; Gustafsson, 2003). Adsorption of both elements has been shown experimentally to be strongly pH-dependent, with Mo more strongly adsorbed at low pH. We therefore speculate that the pH of saprolites controls Mo behavior in the oxidized smectite zone.

Because oxides are known to fractionate Mo isotopes, and are suggested to exist above the redox discontinuity (Liu et al., 2014a, 2014b), one might expect Mo isotopes to be strongly fractionated only in the upper 2 m of the profile. Instead, we observe near constant fractionation throughout, even in the absence of abundant oxides or organic matter below the redox discontinuity. Below the redox discontinuity, kaolinite is the dominant clay species and the saprolites are cut by siderite veins. With the exception of the sample that borders the redox discontinuity, Mo concentrations are quite constant in this region and there is no obvious trend in δ^{98}Mo values, though all are lower than that of the parental rock (Fig. 1). Comparing δ^{98}Mo to other chemical indexes helps to elucidate isotopic fractionation behavior. The δ^{98}Mo values of the samples below the redox discontinuity (light blue in Fig. 3) positively correlate with P_2O_5. Sorption of P_2O_5 and Mo onto the surface of minerals is pH-dependent (Goldberg et al., 1996; Gustafsson, 2003). Thus, the correlation between δ^{98}Mo and P_2O_5 suggests that pH controlled Mo adsorption and isotope fractionation in the kaolinite region. Phosphorous is used as a proxy for pH of the sorption environment; it is more strongly adsorbed at low pH (Gustafsson, 2003), so one can infer that samples with a lower P_2O_5 concentration formed at higher pH. The saprolite data show that samples that retain less phosphate, i.e., formed at higher pH, also have a more strongly fractionated Mo isotope signature (e.g., δ^{98}Mo is lower) compared to the bedrock value (Fig. 3). The inference that Mo is more strongly fractionated at higher pH in the saprolites is consistent with the results of King et al. (2016) and compiled literature data that show an anti-correlation between pH and δ^{98}Mo (Fig. 4).

Additionally, in the lower, kaolinite-dominated region of the saprolite profile, δ^{98}Mo is weakly correlated with δ^{7}Li and density (Fig. 3). Both of these parameters measure the degree of weathering (e.g., isotopically light Li, low density), suggesting that the most weathered samples contain the lowest δ^{98}Mo values. The saprolites contain minor (<2%) opaque minerals which may be Fe-oxides (Gardner, 1981). If present, these oxides may be the fractionating mineral species here since experimental studies show that Mo is much more strongly adsorbed onto oxides than clays (Goldberg et al., 1996), and the leaching studies of Wang et al. (2018, 2020) suggest that oxides control Mo behavior more than clays in saprolites. Thus, we infer that weathering of the diabase

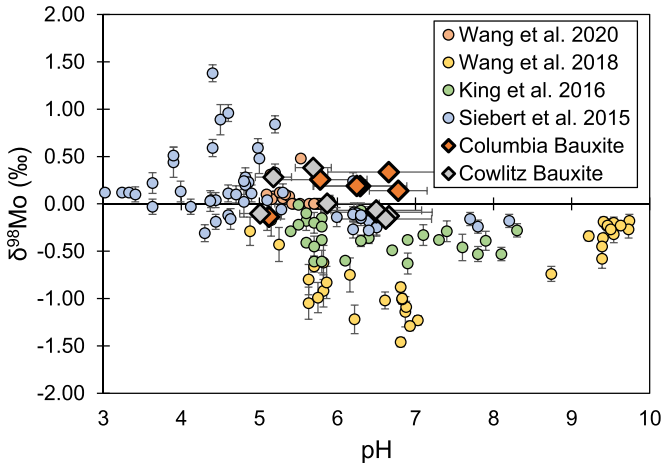

Fig. 4. Relationship between pH and δ^{98}Mo from published studies of soils and saprolites. Data from Siebert et al. (2015), King et al. (2016), Wang et al. (2018), and Wang et al. (2020) are in circles. The two bauxite profiles from this study are plotted as diamonds.

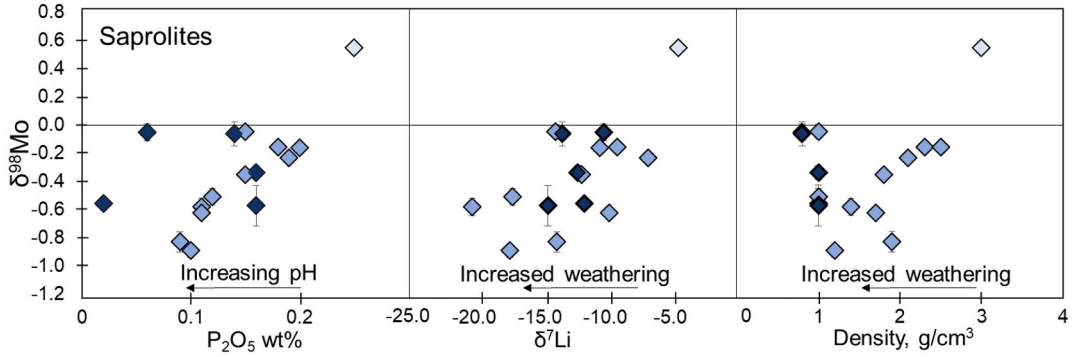

Fig. 3. δ^{98}Mo crossplots with phosphorous concentration, δ^{7}Li, and density to evaluate the effect of progressive weathering and pH on the saprolites. The lightest blue diamond with highest δ^{98}Mo represents the bedrock diabase, the medium shaded blue diamonds represent samples in the kaolinite-dominated region below the redox discontinuity, and samples in the darkest blue are taken from above the redox discontinuity. The P_2O_5, δ^{7}Li, and density data came from Gardner (1981) and Rudnick et al. (2004). The horizontal line denotes δ^{98}Mo of zero. (For interpretation of the references to colour in this figure legend, the reader is referred to the web version of this article.)

resulted in an overall loss of Mo, with isotopically light Mo being selectively retained within the saprolite, likely within primary oxides, or adsorbed to secondary hydroxide minerals.

4.2. Bauxites

The bauxites tell a more complex story than the saprolites. While the saprolites can be explained by a single stage of weathering during which isotopically heavier Mo is preferentially removed from the weathering profile, the bauxite profiles contain significantly more Mo than the bedrock ($\tau_{Mo\text{-}Ti}$ values ranging up to ~4), requiring Mo addition. Additionally, the bauxite profiles show a range of [Mo] and δ^{98}Mo values that correlate with the major mineralogy of the profile: the upper pisolite portion contains more Mo and higher δ^{98}Mo values than either the parent basalts or the lower gibbsite portion. Indeed, even within the pisolite layers of the Columbia profile, [Mo] and δ^{98}Mo correlate with the proportion of pisolites determined by Fassio (1990) (Fig. 1). The pisolites are suggested to have nucleated onto quartz crystals and are primarily composed of hematite, goethite, and minor maghemite (Fassio, 1990). It is unsurprising that these regions of the bauxite profile are enriched in Mo, given Mo's propensity to adsorb onto Fe-oxides (Goldberg et al., 1996). Additionally, the pH of the bauxites ranges 5 to 7 (Fig. 4). This slight acidity likely promotes Mo adsorption onto Fe-oxides, though, Mo isotopes have been experimentally shown to fractionate in the *opposite* direction due to adsorption onto Fe-oxides, i.e., the oxides are expected to attract isotopically light Mo, leaving isotopically heavy Mo in solution (Goldberg et al., 2009). In the bauxite profiles, samples that lie within the pisolite zone have high δ^{98}Mo values, ranging from +0.14 to +0.38‰, which is a + 0.25‰ to +0.67‰ increase relative to parent basalt values.

The retention of isotopically heavy Mo in weathering profiles has been observed during Mo adsorption onto organic matter (King et al., 2016, 2018). Although experiments suggest that organic matter should attract isotopically light Mo (King et al., 2018), studies of topsoil show that increasing proportions of organic matter in soils correlates with increasingly heavier Mo isotopes (King et al., 2016, 2018). King et al. (2018) suggest that infiltration of rainwater provided isotopically heavy Mo that was adsorbed by the organic matter, leaving an overall isotopically heavy signature in the soils. Rainwater is isotopically heavy, with an average δ^{98}Mo value of +1.11‰ in Hawaii and average concentration of 0.007 ppb (King et al., 2016). Groundwater is also isotopically heavy compared to weathered regolith; two studies estimate the average δ^{98}Mo of groundwater to be +0.14‰ and + 0.34‰ with average concentrations of and 3 ppb and 10 ppb (King et al., 2016; Neely et al., 2018, respectively).

Here, we propose that the addition of isotopically heavy groundwater added Mo to the bauxites, resulting in an increase in Mo concentration and a shift to isotopically heavier Mo relative to the parent rock (Fig. 1). It is well established that bauxites form under intense leaching of bedrock caused by abundant rainfall and/or groundwater flow (Schellmann, 1994), and it has been suggested that the bauxite profiles studied here formed within an aquifer (Fassio, 1990). The bedrock surrounding the bauxites studied here is primarily volcanic. Leaching of these igneous rocks could supply ample Mo to the groundwater.

The pisolites that formed in the upper layer of the bauxite profiles likely created fresh surfaces for the near quantitative adsorption of Mo from the groundwater. Fassio (1990) propose that the pisolite layers formed due to a change in climatic conditions from a continuously wet climate to a seasonal wet and dry climate. This seasonality caused the water table to fluctuate, allowing for the concentric growth of Fe-(hydr) oxide pisolites with freshly exposed mineral faces each season. This change from constant lateral fluid flow (lower gibbsite layers) to fluctuating fluid flow over fresh Fe-(hydr)oxide surfaces in the pisolite layer likely provided more sites for Mo (likely as molybdate) adsorption, relative to the oxides in the gibbsite layers.

The repeated exposure of these fresh mineral faces may have quantitatively removed Mo from the groundwater, resulting in adsorption of both isotopically light and heavy Mo. The measured δ^{98}Mo values of groundwater from basalt-rich Iceland and Hawaii (average δ^{98}Mo of +0.14‰ and +0.34‰; King et al., 2016 and Neely et al., 2018) overlaps that observed in the pisolite layer (δ^{98}Mo from +0.14 to +0.38‰). Assuming that published groundwater measurements are representative of the groundwater that flowed through the bauxites, near quantitative removal of Mo from groundwater would be needed to generate equally heavy Mo enrichments in the pisolite layers in the bauxites. Because groundwater contains two to three orders of magnitude more Mo than rainwater (King et al., 2016; Neely et al., 2018), groundwater is likely to be the source of the large Mo enrichments observed in the pisolite layers.

While the Fe-pisolite layers are enriched in Mo and contain heavy Mo isotopes, the lower gibbsite layers are geochemically more similar to the saprolites (Fig. 1). The gibbsite layers have neither gained nor lost significant Mo relative to the parental basalt, and their δ^{98}Mo values vary from the bedrock by Δ^{98}Mo = +0.01 to +0.25‰. Gibbsites in the Cowlitz profile have $\tau^{Mo}{}_{Ti}$ values slightly below zero – indicating slight loss of Mo from the profile – which corresponds well with δ^{98}Mo values that are lower than those of the bedrock. As in the saprolite profile, this implies that Mo is fractionated during weathering, leaving isotopically light Mo in the weathering residue while isotopically heavy Mo is leached from the profile by groundwater.

Previously, Liu et al. (2013) concluded that addition of 20–60 wt% dust to the top of the bauxite profiles added quartz and unradiogenic Nd. However, the addition of dust cannot be the source of the high δ^{98}Mo observed in the upper portions of the profiles because loess has an average δ^{98}Mo identical to estimates of the "primary" igneous continental crust (+0.06 ± 0.17‰; Wang et al., 2018). This does not preclude dust from being added to these profiles, but another, heavier source of Mo (groundwater or rainwater) is also a necessary addition.

4.3. Mo behavior during continental weathering

When the two datasets presented here are combined, the overall Mo isotope behavior during weathering becomes clear. Plotting δ^{98}Mo against both [Mo] and $\tau^{Mo}{}_{Ti}$ of the bedrock and weathered samples reveals a general trend where regolith that has lost Mo during weathering (e.g., saprolites and some gibbsite-bearing bauxites) is isotopically lighter than the bedrock and general estimates of "primary" igneous upper continental crust (UCC) (Fig. 5). On the other hand, soils that have gained Mo – due to a significant abundance of Fe-(hydr)oxides that captured Mo from percolating groundwater or rainwater – are isotopically heavier than the bedrock and average UCC.

When compared to data from a similar study of saprolites by Wang et al. (2018), the same general trend is apparent: when Mo is lost from the saprolites relative to the bedrock, as determined by the $\tau^{Mo}{}_{Ti}$ value, nearly all of the saprolites are isotopically lighter than the bedrock (a granite). Interestingly, Wang et al.'s (2018) data show a negative relationship between $\tau^{Mo}{}_{Ti}$ and δ^{98}Mo, however the weathered samples that lost Mo are still lighter than the granite bedrock, so the overall trend holds. This trend is not as evident in studies of topsoil (King et al., 2016; Siebert et al., 2015), likely because topsoils are much younger and still under the influence of decaying organic matter and atmospheric inputs. Therefore, we find that while such studies generate useful information about Mo behavior during weathering, they do not record trends on the longer timescales of continental weathering like these deeper saprolite and bauxite profiles.

While the bauxites studied here are enriched in Mo and heavy Mo isotopes, bauxites are a relatively rare weathering product, and only form under extreme weathering conditions. Usually these sediments are confined to tropical latitudes and form on more mafic rocks under intense leaching conditions (Schellmann, 1994; Bogatyrev et al., 2009), whereas saprolites are more ubiquitous and form on mafic to felsic rocks (e.g., Wang et al., 2018 and this study). Thus, we consider saprolites to

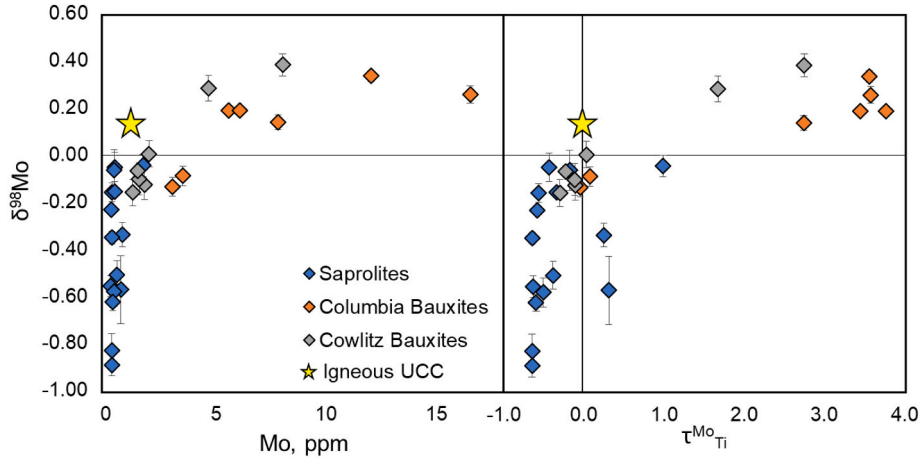

Fig. 5. Trend between δ^{98}Mo and [Mo] and τ_{Mo} for the primary bedrock and weathered samples studied here and for average UCC. Estimates for the igneous upper crust are shown as a star (UCC [Mo] from Rudnick and Gao 2014; δ^{98}Mo estimated from Willbold and Elliott, 2017; Voegelin et al., 2014; Yang et al., 2017).

be more representative of widespread continental weathering. Given this assumption, we conclude that during modern continental weathering, there is a net loss of Mo that leaves the weathered regolith isotopically light and contributes to the isotopically heavy signature observed in rivers (Archer and Vance, 2008; Wang et al., 2018).

Finally, the weathering profile data corroborate the findings of Greaney et al. (2020), who showed that the weathered UCC, as recorded by glacial diamictites, has evolved to isotopically lighter values over time due to increasing atmospheric oxygen levels. Increasing oxidative weathering breaks down Mo-bearing phases like MoS_2 (Johnson et al., 2019), mobilizes Mo, and results in a net Mo loss and isotopic fractionation from upper crustal values. Overall, the limiting factor for Mo loss from the continents and fractionation through time is the amount of O_2 in the atmosphere and surface waters that is available to liberate and transport crustal Mo.

5. Conclusions

The Mo isotopes in a saprolite and two bauxite weathering profiles highlight the "long term" behavior of Mo during different styles of continental weathering. The saprolites, which we consider to represent typical weathering conditions of bedrock given their widespread abundance, show overall Mo loss with preferential retention of light Mo isotopes. By contrast, the bauxites – which represent extreme weathering that is typically restricted to tropical regions with high rainfall, formed on mafic rocks with significant leaching of the profile – record net Mo gain with preferential retention of heavy Mo isotopes. From these data, we conclude that moderate continental weathering results in a loss of Mo from the crust, accompanied by fractionation as light Mo isotopes are absorbed onto minor Fe—Mn (hydr)oxides and clays in the weathering profile. The Mo that is leached from the profile is therefore predicted to be isotopically heavy, which partially explains why groundwater and river water are isotopically heavy (Archer and Vance, 2008; King et al., 2016; Neely et al., 2018). By contrast, the bauxites formed through intense leaching by groundwater represent archives of the predicted heavy Mo isotope composition of groundwater. While Mo may initially be stripped from the bauxite profiles during the early stages of weathering, continual interaction with isotopically heavy groundwater may lead to the adsorption of isotopically heavy Mo onto the abundant Fe-(hydr)oxides (up to 50% of the modal mineralogy) that form in these lithologies.

Declaration of Competing Interest

The authors declare that they have no known competing financial interests or personal relationships that could have appeared to influence the work reported in this paper.

Acknowledgements

We thank Xiao-Ming Liu for providing additional bauxite powders. Two anonymous reviewers provided helpful suggestions to improve the manuscript. This research was supported by funding from the following NSF grants: EAR 133810 (Anbar, PI, Rudnick, co-I); EAR0948549 and EAR1757313 (Rudnick, PI).

Appendix A. Supplementary data

Supplementary data to this article can be found online at https://doi.org/10.1016/j.chemgeo.2021.120103.

References

Anbar, A.D., Duan, Y., Lyons, T.W., Arnold, G.L., Kendall, B., Creaser, R.A., Kaufman, A. J., Gordon, G.W., Scott, C., Garvin, J., Buick, R., 2007. A whiff of oxygen before the great oxidation event? Science 317, 1903–1906. https://doi.org/10.1126/science.1140325.

Archer, C., Vance, D., 2008. The isotopic signature of the global riverine molybdenum flux and anoxia in the ancient oceans. Nat. Geosci. 1, 597–600. https://doi.org/10.1038/ngeo282.

Barling, J., Anbar, A.D., 2004. Molybdenum isotope fractionation during adsorption by manganese oxides. Earth Planet. Sci. Lett. 217, 315–329. https://doi.org/10.1016/S0012-821X(03)00608-3.

Barling, J., Arnold, G.L., Anbar, A.D., 2001. Natural mass-dependent variations in the isotopic composition of molybdenum. Earth Planet. Sci. Lett. 193, 447–457. https://doi.org/10.1016/S0012-821X(01)00514-3.

Bogatyrev, B.A., Zhukov, V.V., Tsekhovsky, Y.G., 2009. Formation Conditions and Regularities of the Distribution of Large and Superlarge Bauxite Deposits, 44, pp. 135–151. https://doi.org/10.1134/S0024490209020035.

Chappaz, A., Lyons, T.W., Gregory, D.D., Reinhard, C.T., Gill, B.C., Li, C., Large, R.R., 2014. Does pyrite act as an important host for molybdenum in modern and ancient euxinic sediments? Geochim. Cosmochim. Acta 126, 112–122. https://doi.org/10.1016/j.gca.2013.10.028.

Chen, H., Liu, X.M., Wang, K., 2020. Potassium isotope fractionation during chemical weathering of basalts. Earth Planet. Sci Lett. 539, 116192. https://doi.org/10.1016/j.epsl.2020.116192.

Dahl, T.W., Chappaz, A., Hoek, J., McKenzie, C.J., Svane, S., Canfield, D.E., 2017. Evidence of molybdenum association with particulate organic matter under sulfidic conditions. Geobiology 15, 311–323. https://doi.org/10.1111/gbi.12220.

Duan, Y., Anbar, A.D., Arnold, G.L., Lyons, T.W., Gordon, G.W., Kendall, B., 2010. Molybdenum isotope evidence for mild environmental oxygenation before the Great Oxidation Event. Geochim. Cosmochim. Acta 74, 6655–6668. https://doi.org/10.1016/j.gca.2010.08.035.

Fassio, J.M., 1990. Geochemical Evolution of Ferrginous Bauxite Deposits in Northwestern Oregon and Southwestern Washington. MS Thesis. Portland State University, p. 103.

Gardner, L.R., 1981. Geochemistry and mineralogy of an unusual diabase saprolite near Columbia, South Carolina. Clays Clay Miner. 29, 184–190. https://doi.org/10.1346/CCMN.1981.0290303.

Gaschnig, R.M., Rudnick, R.L., McDonough, W.F., Kaufman, A.J., Hu, Z., Gao, S., 2014. Onset of oxidative weathering of continents recorded in the geochemistry of ancient glacial diamictites. Earth Planet. Sci. Lett. 408, 87–99. https://doi.org/10.1016/j.epsl.2014.10.002.

Goldberg, S., Forster, H.S., Godfrey, C.L., 1996. Molybdenum adsorption on oxides, clay minerals, and soils. Soil Sci. Soc. Am. J. 60, 425. https://doi.org/10.2136/sssaj1996.03615995006000020013x.

Goldberg, T., Archer, C., Vance, D., Poulton, S.W., 2009. Mo isotope fractionation during adsorption to Fe (oxyhydr)oxides. Geochim. Cosmochim. Acta 73, 6502–6516. https://doi.org/10.1016/j.gca.2009.08.004.

Greaney, A.T., Rudnick, R.L., Romaneillo, S., Johnson, A.C., Gaschnig, R.M., Anbar, A.D., 2020. Molybdenum isotope fractionation in glacial diamictites tracks the onset of oxidative weathering of the continental crust. Earth Planet. Sci. Lett. 534 https://doi.org/10.1016/j.epsl.2020.116083.

Gustafsson, J.P., 2003. Modelling molybdate and tungstate adsorption to ferrihydrite. Chem. Geol. 200, 105–115. https://doi.org/10.1016/S0009-2541(03)00161-X.

Johnson, A.C., Romaniello, S.J., Reinhard, C.T., Gregory, D.D., Garcia-Robledo, E., Revsbech, N.P., Canfield, D.E., Lyons, T.W., Anbar, A.D., 2019. Experimental determination of pyrite and molybdenite oxidation kinetics at nanomolar oxygen concentrations. Geochim. Cosmochim. Acta 249, 160–172. https://doi.org/10.1016/j.gca.2019.01.022.

Kendall, B., Dahl, T.W., Anbar, A.D., 2017. The stable isotope geochemistry of molybdenum. Rev. Miner. Geochem. 82, 683–732. https://doi.org/10.2138/rmg.2017.82.16.

King, E.K., Thompson, A., Chadwick, O.A., Pett-Ridge, J.C., 2016. Molybdenum sources and isotopic composition during early stages of pedogenesis along a basaltic climate transect. Chem. Geol. 445, 54–67. https://doi.org/10.1016/j.chemgeo.2016.01.024.

King, E.K., Perakis, S.S., Pett-Ridge, J.C., 2018. Molybdenum isotope fractionation during adsorption to organic matter. Geochim. Cosmochim. Acta 222, 584–598. https://doi.org/10.1016/j.gca.2017.11.014.

Kohn, M.J., Miselis, J.L., Fremd, T.J., 2002. Oxygen isotope evidence for progressive uplift of the Cascade Range, Oregon. Earth Planet. Sci. Lett. 204, 151–165.

Liu, X.M., Rudnick, R.L., McDonough, W.F., Cummings, M.L., 2013. Influence of chemical weathering on the composition of the continental crust: insights from Li and Nd isotopes in bauxite profiles developed on Columbia River Basalts. Geochim. Cosmochim. Acta 115, 73–91. https://doi.org/10.1016/j.gca.2013.03.043.

Liu, S.A., Teng, F.Z., Li, S., Wei, G.J., Ma, J.L., Li, D., 2014a. Copper and iron isotope fractionation during weathering and pedogenesis: insights from saprolite profiles. Geochim. Cosmochim. Acta 146, 59–75. https://doi.org/10.1016/j.gca.2014.09.040.

Liu, X.M., Teng, F.Z., Rudnick, R.L., McDonough, W.F., Cummings, M.L., 2014b. Massive magnesium depletion and isotope fractionation in weathered basalts. Geochim. Cosmochim. Acta 135, 336–349. https://doi.org/10.1016/j.gca.2014.03.028.

Marks, J.A., Perakis, S.S., King, E.K., Pett-Ridge, J., 2015. Soil organic matter regulates molybdenum storage and mobility in forests. Biogeochemistry 125, 167–183. https://doi.org/10.1007/s10533-015-0121-4.

Neely, R.A., Gislason, S.R., Ólafsson, M., McCoy-West, A.J., Pearce, C.R., Burton, K.W., 2018. Molybdenum isotope behaviour in groundwaters and terrestrial hydrothermal systems, Iceland. Earth Planet. Sci. Lett. 486, 108–118. https://doi.org/10.1016/j.epsl.2017.11.053.

Ostrander, C.M., Nielsen, S.G., Owens, J.D., et al., 2019. Fully oxygenated water columns over continental shelves before the Great Oxidation Event. Nat. Geosci. 12, 186–191. https://doi.org/10.1038/s41561-019-0309-7.

Pearce, C.R., Burton, K.W., von Strandmann, P.A.E.P., James, R.H., Gíslason, S.R., 2010. Molybdenum isotope behaviour accompanying weathering and riverine transport in a basaltic terrain. Earth Planet. Sci. Lett. 295, 104–114. https://doi.org/10.1016/j.epsl.2010.03.032.

Romaniello, S.J., Herrmann, A.D., Anbar, A.D., 2016. Syndepositional diagenetic control of molybdenum isotope variations in carbonate sediments from the Bahamas. Chem. Geol. 438, 84–90. https://doi.org/10.1016/j.chemgeo.2016.05.019.

Rudnick, R.L., Tomascak, P.B., Njo, H.B., Gardner, L.R., 2004. Extreme lithium isotopic fractionation during continental weathering revealed in saprolites from South Carolina. Chem. Geol. 212, 45–57. https://doi.org/10.1016/j.chemgeo.2004.08.008.

Rudnick, R.L., Gao, S., 2014. Composition of the Continental Crust. In: Holland, H.D., Turekian, K.K. (Eds.), Treatise on Geochemistry, Second edition, 4. Elsevier. Chapter: 1.

Schellmann, W., 1994. Geochemical Differentiation in Laterite and Bauxite Formation, 21, pp. 131–143.

Scott, C., Lyons, T.W., Bekker, A., Shen, Y., Poulton, S.W., Chu, X., Anbar, A.D., 2008. Tracing the stepwise oxygenation of the Proterozoic Ocean. Nature 452, 456–459. https://doi.org/10.1038/nature06811.

Siebert, C., Nägler, T.F., von Blanckenburg, F., Kramers, J.D., 2003. Molybdenum isotope records as a potential new proxy for paleoceanography. Earth Planet. Sci. Lett. 211, 159–171. https://doi.org/10.1016/S0012-821X(03)00189-4.

Siebert, C., Kramers, J.D., Meisel, T., Morel, P., Nägler, T.F., 2005. PGE, Re-Os, and Mo isotope systematics in Archean and early Proterozoic sedimentary systems as proxies for redox conditions of the early Earth. Geochim. Cosmochim. Acta 69 (7), 1787–1801.

Siebert, C., Pett-Ridge, J.C., Opfergelt, S., Guicharnaud, R.A., Halliday, A.N., Burton, K.W., 2015. Molybdenum isotope fractionation in soils: influence of redox conditions, organic matter, and atmospheric inputs. Geochim. Cosmochim. Acta 162, 1–24. https://doi.org/10.1016/j.gca.2015.04.007.

Teng, F.Z., Li, W.Y., Rudnick, R.L., Gardner, L.R., 2010. Contrasting lithium and magnesium isotope fractionation during continental weathering. Earth Planet. Sci. Lett. 300, 63–71. https://doi.org/10.1016/j.epsl.2010.09.036.

Teng, F.-Z., Hu, Y., Ma, J.-L., Wie, G.-J., Rudnick, R.L., 2020. Potassium isotope fractionation during continental weathering and implications for global K isotopes balance. Geochim. Cosmochim. Acta 278, 261–271. https://doi.org/10.1016/j.gca.2020.02.029.

Voegelin, A.R., Pettke, T., Greber, N.D., von Niederhäusern, B., Nägler, T.F., 2014. Magma differentiation fractionates Mo isotope ratios: evidence from the Kos Plateau Tuff (Aegean Arc). Lithos 190–191, 440–448. https://doi.org/10.1016/j.lithos.2013.12.016.

Wang, Z., Ma, J., Li, J., Wei, G., Zeng, T., Li, L., Zhang, L., Deng, W., Xie, L., Liu, Z., 2018. Fe (hydro) oxide controls Mo isotope fractionation during the weathering of granite. Geochim. Cosmochim. Acta 226, 1–17. https://doi.org/10.1016/j.gca.2018.01.032.

Wang, Z., Ma, J., Li, J., Zeng, T., Zhang, Z., He, X., Zhang, L., Wei, G., 2020. Effect of Fe–Ti oxides on Mo isotopic variations in lateritic weathering profiles of basalt. Geochim. Cosmochim. Acta 286, 380–403.

Wasylenki, L.E., Rolfe, B.A., Weeks, C.L., Spiro, T.G., Anbar, A.D., 2008. Experimental investigation of the effects of temperature and ionic strength on Mo isotope fractionation during adsorption to manganese oxides. Geochim. Cosmochim. Acta 72, 5997–6005. https://doi.org/10.1016/j.gca.2008.08.027.

Wichard, T., Mishra, B., Myneni, S.C.B., Bellenger, J.P., Kraepiel, A.M.L., 2009. Storage and bioavailability of molybdenum in soils increased by organic matter complexation. Nat. Geosci. 2, 625–630. https://doi.org/10.1038/ngeo589.

Willbold, M., Elliott, T., 2017. Molybdenum isotope variations in magmatic rocks. Chem. Geol. 449, 253–268. https://doi.org/10.1016/j.chemgeo.2016.12.011.

Wille, M., Kramers, J.D., Nagler, T.F., Beukes, N.J., Schroder, S., Meisel, T.H., Lacassie, J.B., Voegelin, A.R., 2007. Evidence for a gradual rise of oxygen between 2.6 and 2.5 Ga from Mo isotopes and Re-PGE signatures in shales. Geochim. Cosmochim. Acta 71, 2417–2435.

Wille, M., Nebel, O., Van Kranendonk, M.J., Schoenberg, R., Kleinhanns, I.C., Ellwood, M.J., 2013. Mo-Cr isotope evidence for a reducing Archean atmosphere in 3.46-2.76Ga black shales from the Pilbara, Western Australia. Chem. Geol. 340, 68–76. https://doi.org/10.1016/j.chemgeo.2012.12.018.

Yang, J., Barling, J., Siebert, C., Fietzke, J., Stephens, E., Halliday, A.N., 2017. The molybdenum isotopic compositions of I-, S- and A-type granitic suites. Geochim. Cosmochim. Acta 205, 168–186. https://doi.org/10.1016/j.gca.2017.01.027.